

## Structural and Kinetic Factors Governing the Formation of the $\gamma$ Polymorph of Isotactic Polypropylene

Rufina G. Alamo\* and Man-Ho Kim

Department of Chemical Engineering, Florida Agricultural and Mechanical University, and Florida State University College of Engineering, 2525 Pottsdamer St., Tallahassee, Florida 32310-6046

María J. Galante,<sup>†</sup> José R. Isasi, and Leo Mandelkern\*

Department of Chemistry and Institute of Molecular Biophysics, Florida State University, Tallahassee, Florida 32306-4380

Received November 30, 1998; Revised Manuscript Received March 29, 1999

**ABSTRACT:** The molecular, thermodynamic, and kinetic factors that govern the formation and concentration of the  $\alpha$  and  $\gamma$  polymorphs in metallocene-catalyzed isotactic poly(propylenes) have been studied with a set of polymers that have a wide range in molecular weight and defect contents. With these polymers it was possible to investigate the influence of molecular weight on  $\gamma$  formation at a fixed defect concentration, as well as the role of the defect concentration at constant molecular weight. The major experimental techniques used were wide-angle X-ray scattering and differential scanning calorimetry complemented by microscopy. From these studies the role of chain microstructure, the crystallization temperature, and the thermodynamic and kinetic requirement for the formation of the  $\gamma$  form could be established in more quantitative detail than heretofore. A particular important finding was the fact that at fixed defect concentration the fractional content of the  $\gamma$  polymorph goes through a maximum with crystallization temperature. The results that were obtained establish a quantitative framework within which the underlying bases that lead to formation of the  $\gamma$  form, and its unique crystalline structure, are discussed.

### Introduction

Isotactic poly(propylene) possesses some features that are unique to a semicrystalline polymer. This polymer exhibits three different, well-defined, crystallographic forms. The chain conformation of each is in the classical  $3_1$  helix. The difference in the crystallography is the manner in which the chains are packed in the unit cell. The crystallographic habits of the three polymorphs have recently been reviewed in detail.<sup>1</sup> The most commonly observed crystal form is the monoclinic or  $\alpha$  form. The lamellar morphology associated with this crystallographic form is unusual. Transversal lamellae grow epitaxially from those initially formed, giving a mesh-type crosshatched morphology.<sup>2</sup> Details of this lamellar structure and its influence on thermodynamic properties have been reported in detail.<sup>3</sup> The  $\beta$  or hexagonal form is found either after crystallization under stress or by adding specific nucleating agents to quiescent melts. The  $\beta$  form transforms to the  $\alpha$  form on heating. Early X-ray diffraction studies of the third polymorph, the  $\gamma$  form, concluded that this crystallographic form was triclinic.<sup>4,5</sup> However, more recent work has determined that this polymorph is in fact orthorhombic.<sup>6–8</sup> The structure of the orthorhombic unit cell of the  $\gamma$  form is unprecedented for polymeric systems. It represents the first, if not the only, one to date, wherein the chain axes are nonparallel to one another. In this structure parallel helices, two chains wide, are tilted  $80^\circ$  with respect to another in an adjacent bilayer. The present work focuses attention on the conditions for the formation of the  $\gamma$  polymorph and its properties. Of particular interest is

the role played by the chain microstructure and the crystallization temperature.

In early work, using Ziegler–Natta catalysts, the  $\gamma$  form was obtained by either crystallization of high molecular weight species at elevated pressures,<sup>9–13</sup> crystallization at atmospheric pressure of very low molecular weight chains,<sup>14–17</sup> or crystallizing propylene copolymers.<sup>18–21</sup> It is difficult, however, to develop meaningful correlations between molecular structure and properties of the isotactic poly(propylenes) prepared with this catalyst. The reason is that chain length and stereo defect composition are inversely related to one another.<sup>22–25</sup> The low molecular weights contain a high concentration of chain defects while the microstructures of the high molecular weights approach that of the stereoregular chain. The low molecular weight fractions that were used to obtain the  $\gamma$  form thus contained a high concentration of defects.<sup>6,7</sup> It has been speculated that interruptions in the regular sequences of isotactic poly(propylene) favored the development of the  $\gamma$  form.<sup>1</sup>

Metallocene-catalyzed isotactic poly(propylene) yields polymers that have most probable molecular weight distributions ( $M_w/M_n \approx 2$ ) and narrow composition distributions. The study of this type polymer allows for the molecular length and defect concentration to be varied independently. Thus, the relation between chain length, defect concentration, and the formation of the  $\gamma$  polymorph can be studied. In addition to the conventional stereo-type defect, metallocene-catalyzed isotactic poly(propylene) chains also contain regio defects. Several studies of  $\gamma$  formation in this type of isotactic poly(propylene) have been reported.<sup>6,26–29a,b</sup> In one, the fraction of the  $\gamma$  structure that develops in a relatively low molecular weight polymer,  $M_w = 18\,000$  g/mol, with a high defect concentration was studied as a function

<sup>†</sup> Present address: INTEMA, Juan B. Justo 4302, Mar del Plata (7600), Argentina.

\* To whom correspondence should be addressed.

**Table 1. Molecular Characterization of Metallocene Poly(propylenes) with Constant Concentration of Defects**

samples	$M_w$	$M_w/M_n$	isotactic <sup>a</sup> [mmmm]	stereo defects (%)	regio <sup>b</sup> defects (%)	total defects (mol %)	$\eta_{iso}$ <sup>d</sup>
M41K	41 260	2.1					
M68K 1.57	68 480	2.1	0.940	0.97	0.60	1.57	58
M69K 1.70	69 190	2.1	~0.95	~0.90	~0.80	~1.70	54
M142K 1.70	142 000 <sup>c</sup>	~2	~0.95	~0.90	~0.80	~1.70	56
M170K 1.70	169 800	1.8	~0.95	~0.90	~0.80	~1.70	56
M288K 1.69	288 430	1.8	0.954	0.83	0.86	1.69	57

<sup>a</sup> Fraction of isotactic pentads measured from <sup>13</sup>C NMR. <sup>b</sup> 2, 1 additions (erythro). <sup>c</sup> Interpolated from intrinsic viscosity/ $M_w$  relation. <sup>d</sup> From eq 1.

**Table 2. Molecular Characterization of Metallocene Poly(propylenes) with a Constant Low Content of Mainly 2,1 Additions**

sample	$M_w$	$M_w/M_n$	[mmmm]	stereo (%)	regio <sup>a</sup> 2,1 (%)	total defects (mol %)	$\eta_{iso}$
M102K 0.42	102 500	2.3	0.9959	0.06	0.36	0.42	194
M182K 0.40	182 000	2.0	0.9960	0	0.40	0.40	223
M200K 0.41	200 500	2.0	0.9925	0.01	0.40	0.41	220
M327K 0.41	327 000	2.2	0.9959	0	0.41	0.41	227
M403K 0.41	403 500	2.3	0.9959	0	0.41	0.41	230
M439K 0.39	439 000	2.1	0.9961	0.06	0.33	0.39	243

<sup>a</sup> 2,1 additions (erythro type).

**Table 3. Molecular Characterization of Metallocene Poly(propylenes) with Different Concentration of Defects**

sample	$M_w$	$M_w/M_n$	[mmmm]	stereo defects (%)	regio 2-1 (%)	regio 1-3 (%)	total defects (mol %)	$\eta_{iso}$
M575K 0.30	575 500	2.4	0.995	0.08	0.22	0	0.30	314
M200K 0.41	200 500	2.0	0.9925	0.01	0.40	0	0.41	220
M349K 0.44	349 500	2.5	0.991	0.09	0.35	0	0.44	212
M346K 1.00	346 500	2.3	0.954	0.84	0.16	0	1.00	96
M236K 1.17	236 400	~2		0.22	0.95	0	1.17	82
M288K 1.69	288 430	1.8	0.954	0.83	0.86	0	1.69	57
M335K 2.35	335 500	2.3	0.908	1.68	0.53	0.14	2.35	41

of the crystallization temperature.<sup>28</sup> In the other, the molecular weight of the samples ranged from 10 000 to 62 000 with a wide range in stereo and regio defects.<sup>29</sup> However, slow cooling from the melt was the only crystallization condition used. These works, although significant, do not allow for an analysis of the wide range of molecular weights, microstructure, and crystallization temperatures that are available.

In the present work, studies were carried out under atmospheric pressure, with metallocene-catalyzed isotactic poly(propylenes) that encompassed a range in molecular weights and defect content that were much greater than previously reported. With this set of polymers it was possible to investigate in a systematic manner the effect of molecular weight on  $\gamma$  formation at fixed defect concentration as well as the role of defect concentration when the molecular weight is held constant. By studying isothermal crystallization kinetics, the relative rates of the formation of the  $\alpha$  and  $\gamma$  polymorphs could be determined as well as the amounts that are formed under specified conditions. From this work the role of chain microstructure and the thermodynamic and kinetic requirements for the formation of the  $\gamma$  form could be established in more quantitative detail than heretofore. The extensive results that are reported establish a framework within which to discuss the underlying basis for the development of this polymorph. It enables one to address the fundamental question as to the driving force(s) that lead to the unique crystalline structure. We limit consideration here to chains that only contain regio and stereo defects. The role of comonomers, when inserted in the chain, will be discussed in a subsequent paper.

## Experimental Section

**Materials.** Three different series of metallocene poly(propylenes) were studied. The effect of the molecular weight

and crystallization temperature on the formation of the  $\gamma$  phase was examined with the two sets of polymers listed in Tables 1 and 2. The samples are designated by molecular weight and defect concentration. Thus, in Table 1, M68K 1.57 represents a metallocene poly(propylene) with  $M_w = 68$  000 and 1.57% defects. The polymers listed in Table 1 have a constant defect concentration of about 1.7 mol of defects per 100 monomeric units, while the molecular weights vary from  $M_w \sim 40$  000 to  $\sim 300$  000 g/mol. The molecular weight distribution is narrow, characteristic of this type of poly(propylene),  $M_w/M_n \approx 2.0$ . Of the total defects, about half are of the stereo type while the remainder are of the 2,1 type of addition. The total defect content is also constant for the series of polymers listed in Table 2. However, the concentration is much lower than for the series listed in Table 1. All of the polymers in this series contain about 0.4 defects per 100 monomeric units. The defects in this series are mainly of the 2,1 type of additions. In some of these polymers the stereo defect content was below the detectable level (about 0.02%). The molecular weights vary from about 100 000 to 439 000 g/mol. The polymers listed in Table 3 were used to study the effect of defect concentration on the formation of the  $\gamma$  phase. Thus, in this series, the molecular weight and molecular weight distribution are approximately constant, and the total amount of structural irregularities (listed as total defect content in the table) varied from 0.3 to 2.34 mol %. The different types of stereo and/or regio defects are also listed. We thus have available a much wider range in molecular weights of metallocene-type isotactic poly(propylenes) that have been studied, heretofore, as well as a significant concentration range in both stereo and regio defects.

Although the major focus of this work is with the metallocene isotactic poly(propylenes) we have, for comparative purposes, also studied two unfractionated Ziegler-Natta catalyzed polymers. Their molecular characteristics are given in Table 4. These polymers only contain stereo defects that are broadly distributed.

In addition to the amount and type of defect, the molecular weight, the polydispersity, and the fraction of isotactic pentads, measured by <sup>13</sup>C NMR, are also listed in the tables.

**Table 4. Molecular Characteristics of Ziegler–Natta Poly(propylenes)**

sample	$M_w$	$M_w/M_n$	mmmm	mmmr/2	$n_{iso}$
A <sup>a</sup>	271 500	6.10	0.9457	0.0086	116
B <sup>a</sup>	312 300	4.5	0.9395	0.0102	98

<sup>a</sup> After removal of atactic fraction (see text).

Crystallizations from the melt at temperatures higher than about 80 °C were carried out in thermostated oil baths. In these experiments, films approximately 20 mm long, 13 mm wide, and 0.5 mm thick were used. The samples were sandwiched between thin aluminum plates and melted in an oil bath at 200 °C for 15 min and then rapidly transferred to another oil bath set at the required crystallization temperature. To prevent degradation during crystallizations that required over 1000 min, the molded plates were placed in vacuum-sealed tubes. After the required crystallization time elapsed, the tubes were quenched in an ice/water bath. Quenching to ice/water or rapid crystallization of the samples from the melt was carried out directly from the hot press to the quenching bath.

**Techniques.** The chain structure was characterized by high-resolution <sup>13</sup>C NMR following assignments previously reported.<sup>30–32</sup> The concentration of stereo defects was calculated from the mmmr pentads as mmmr/2. The fractional content of 2,1 or 1,3 additions was computed from their respective assigned resonances.<sup>33–38</sup> The <sup>13</sup>C NMR spectra were obtained in polypropylenes free of atactic fraction to avoid complications in analyzing the spectra from overlapping peaks. To separate the atactic fraction, the polymer was dissolved in tetrachlorobenzene (2% w/v) and allowed to crystallize by slowly cooling the solution to room temperature. The average length of isotactic sequences between any two structural irregularities in the chain,  $n_{iso}$ , is a quantity of strong interest. It is defined as the number of isotactic monomeric units divided by the number of isotactic sequences. By assuming a random distribution of defects it can be approximated by

$$n_{iso} = \frac{DP - DP \left[ \frac{mmmr}{2} + \text{regio}(2,1) + \text{regio}(1,3) \right]}{1 + DP \left[ \frac{mmmr}{2} + \text{regio}(2,1) + \text{regio}(1,3) \right]} \quad (1)$$

where DP is the degree of polymerization and mmmr/2, regio(2,1), and regio(1,3) are the fractional contents of stereo, 2,1, and 1,3 additions. The isotacticity content and molecular weight of the polymers studied here are high. Therefore, the  $n_{iso}$  values calculated according to eq 1 are basically identical to the average meso run length calculated from the fraction of triads, tetrads, or pentads as derived by Randall.<sup>39</sup> Under these conditions  $\bar{n} = n_{iso} = 1/\text{fractional content of defects}$ . The  $n_{iso}$  values for the polymers studied here are listed in Tables 1–4.

The melting behavior was studied with a Perkin-Elmer DSC-2B differential scanning calorimeter operated at a heating rate of 10 °C/min. The enthalpies of fusion were converted to degrees of crystallinity  $((1 - \lambda)_{\Delta H})$  by taking the enthalpy of fusion of a perfectly crystalline poly(propylene) as 50 cal/g<sup>40</sup> and using indium as standard. The crystallization kinetics were also studied by DSC following the increase in the endothermic peak areas with time.<sup>41</sup>

The wide-angle X-ray scattering patterns (WAXS) were obtained using a slit-collimated Siemens D-500 diffractometer operating in a  $2\theta$  range between 4° and 40°. The instrument is equipped with a removable high-temperature stage. Filtered Cu K $\alpha$  radiation was used as source. The peak assignments of the  $\gamma$  phase, given by Brückner and Meille,<sup>6</sup> were followed. The Miller index assignments given by Turner-Jones<sup>5</sup> were used for the  $\alpha$  phase. As an example, a diffractogram of an isotactic poly(propylene) that contains approximately equal amounts of  $\alpha$  and  $\gamma$  phases is shown in Figure 1. The most characteristic reflection of the  $\gamma$  form is the (117) that appears at a  $2\theta$  of 20.05°. The characteristic peak of the  $\alpha$  form is the

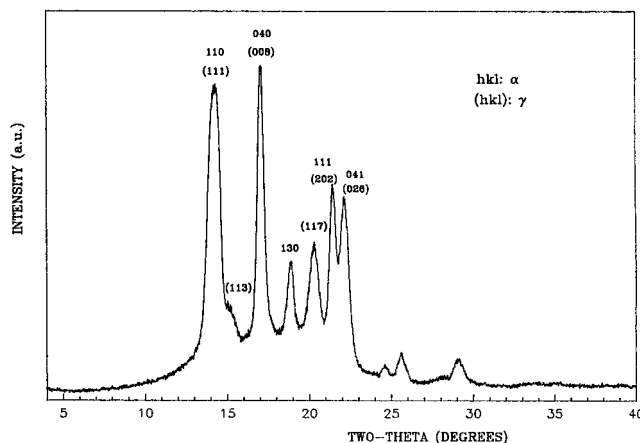


**Figure 1.** WAXS diffractogram of sample M142 K1.70 crystallized at 125 °C. The Miller indexes of the  $\gamma$  phase<sup>6</sup> given in parentheses and of the  $\alpha$  phase<sup>5</sup> are indicated.

(130) index that appears at  $2\theta$  equals 18.8°. The fraction of the  $\gamma$  phase in the crystalline region was obtained from the diffractograms following the method given by Turner-Jones.<sup>18</sup> It was calculated from the heights of the peaks at 18.8° ( $H_\gamma$ ) and 20.05° ( $H_\alpha$ ) as  $(H_\gamma/(H_\gamma + H_\alpha))$ .

## Results and Discussion

### Effect of Varying Molecular Weight for a Fixed Content of Defects.

The effect of molecular weight on the formation of the  $\gamma$  form, at a fixed chain (stereo or regio) defect content, is analyzed with the set of isotactic poly(propylenes) listed in Table 1. Each of the polymers was isothermally crystallized in the temperature interval between 100 and 150 °C and then rapidly transferred to room temperature. The time required to obtain complete transformation at the highest crystallization temperatures was estimated from a previous study of the crystallization kinetics of the same samples.<sup>41</sup> The WAXS measurements were made at room temperature.

The percentage of crystals that develop as the  $\gamma$  polymorph as a function of crystallization temperature for these polymers, after complete crystallization, is given in Figure 2. As the crystallization temperature is raised above 90 °C, the  $\gamma$  form begins to develop at the expense of the  $\alpha$ . In the crystallization temperature interval from 60 to 130 °C the  $\gamma$  fraction increases from 0 to about 60%. Crystallization at 100 °C yielded a relatively small amount of  $\gamma$  content, between 16% and 28%. An extrapolation of the low-temperature side of Figure 2 indicates that at a crystallization temperature of about 90 °C, and below, the  $\gamma$  form will not develop in this molecular weight range for polymers having about 1.7 mol % defects. Experiments show that after rapid crystallization from the melt, to either 23 or 60 °C, only the  $\alpha$  form is observed. A maximum in the  $\gamma$  concentration is reached at about 130 °C, with a continuous decrease being observed above this crystallization temperature. No definitive trend in the  $\gamma$  content could be discerned with molecular weight.

An increase in the  $\gamma$  content with increasing temperature has also been reported for another metallocene-type isotactic poly(propylene).<sup>28</sup> This polymer had a relatively low molecular weight ( $M_w = 18\,000$  g/mol) and a defect content greater than 4.4 mol % and was crystallized under atmospheric pressure.<sup>42</sup> At crystallization temperatures between 115 and 125 °C, this sample crystallized almost completely in the  $\gamma$  form. Crystallizations were not carried out at higher temperatures with this polymer.



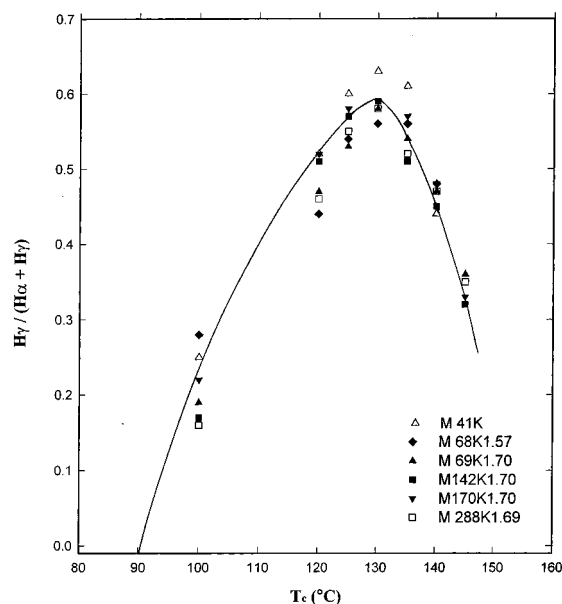


**Figure 2.** Fractional content of the  $\gamma$  polymorph in the crystalline region as a function of crystallization temperature for metallocene poly(propylenes) with the indicated molecular weights.

The observation of a maximum in the plot shown in Figure 2 is both unique and important. Therefore, its validity needs to be carefully examined and substantiated. In general, the crystallization rate of all polymers decrease markedly with increasing temperature at the right side of the maximum of the crystallization rate/temperature plot. Although the time scale of the crystallization was established from earlier crystallization kinetic studies,<sup>41</sup> there could be concern that the decrease in the concentration of the  $\gamma$  polymorph at the higher crystallization temperatures could be the result of an incomplete transformation. Any potential crystallizable material would crystallize upon quenching and contribute to the WAXS pattern. Quenching peaks do not appear in the DSC thermograms for samples crystallized at 130 °C and below. However, after crystallization at temperatures at the right side of the maximum, > 130 °C, in addition to the main endotherm, which corresponds to the melting of the crystallites formed isothermally, a small peak with about 6% crystallinity is also observed at much lower temperatures, about 135 °C. Attempts to eliminate the quenching peak by prolonged crystallization at 135 °C were unsuccessful. Since the WAXS determination of the  $\gamma$  fraction was carried out at room temperature, it is important to determine the crystal form of the quenched crystallites because these crystallites contribute to the WAXS pattern. Our interest, however, is the  $\gamma$  fraction in the crystalline region developed at the crystallization temperature. If the material that crystallized upon quenching did so as  $\alpha$  crystals, then the fractional content of the  $\gamma$  polymorph at the crystallization temperature would increase when these crystals are melted. In this case the maximum observed in Figure 2 would not be meaningful. On the other hand, if the quenched material were composed of  $\gamma$  crystals, then the maximum would be correct. Therefore, these possibilities were examined in more detail.

Figure 3a shows the DSC thermogram of sample M142K 1.70 that was crystallized at 145 °C for about 1 week and then quenched to 23 °C. A broad quenching

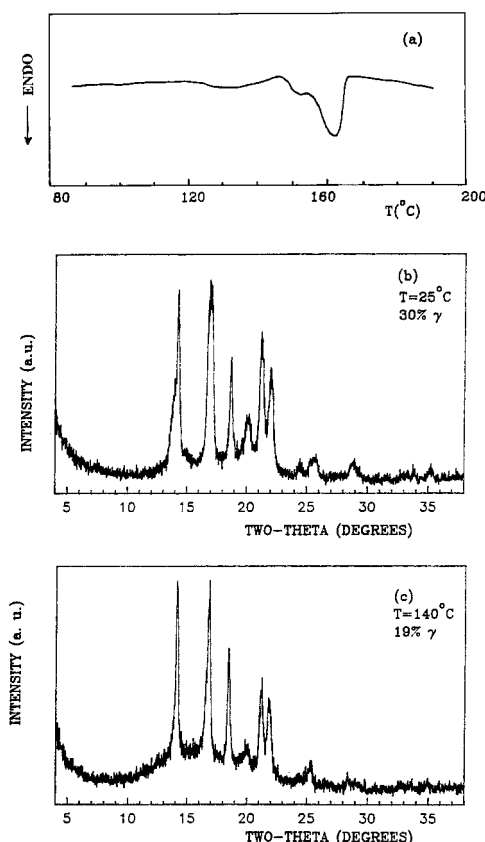


**Figure 3.** (a) DSC melting of sample M142K 1.70 crystallized at 145 °C. The broad melting peak at ~135 °C is due to crystallites formed on quenching. (b, c) WAXS diffractograms of the same sample obtained at 25 °C (b) and at 140 °C (c). Note the decrease of the  $\gamma$  reflection at  $2\theta = 20.05^\circ$  in the lower diffractogram.

peak (130–140 °C) appears in the thermogram together with the two melting peaks of the crystals formed isothermally. Parts b and c of Figure 3 give the WAXS diffractograms of this sample at room temperature and at 140 °C, respectively. The 140 °C temperature is above the melting of the crystals formed on quenching but below those formed isothermally. The intensity of the reflection assigned to the  $\alpha$  polymorph is the same at 140 °C as at room temperature. However, the intensity of the reflection corresponding to the  $\gamma$  form decreases from room temperature to 140 °C. This result indicates that crystals of the  $\gamma$  polymorph are formed on quenching and, therefore, do not have a negative effect in the calculation of the  $\gamma$  content of the samples crystallized at high temperatures. A similar experiment with sample M170K 1.70 crystallized at 140 °C gave identical results; i.e., the crystals formed on quenching are of the  $\gamma$  polymorph. Thus, the decrease in the relative content of the  $\gamma$  phase formed in this series of poly(propylenes) at crystallization temperatures above 130 °C is confirmed.

Support for the maximum in Figure 2 is also found in the following observations derived from the melting behavior. As mentioned previously, all of the polymers in this series that were crystallized above 130 °C give a small quenching peak of approximately the same area that correspond to 5–10% crystallinity. An example is shown in Figure 4 of two thermograms of sample M41K that was crystallized at 135 and 140 °C. The degrees of crystallinity of about 42% are similar for both of the major endotherms. The crystallinity levels of small

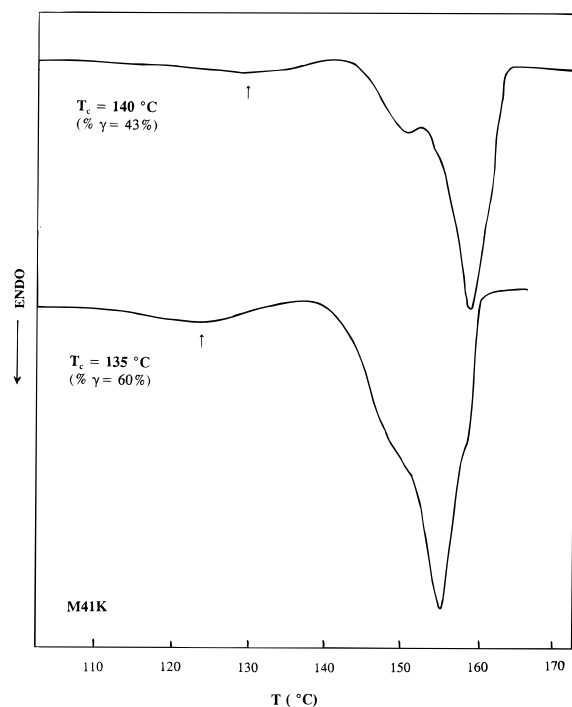


**Figure 4.** DSC endotherms of sample M41K crystallized at 140 °C (top) and 135 °C (lower). These temperatures are in the right side of the maximum of Figure 2. The fractional content of  $\gamma$  crystals formed is significantly different although the broad endotherm formed from quenching is similar.

quenching peaks are also similar. However, the WAXS measurements at room temperature indicate that the  $\gamma$  fraction of the sample crystallized at 140 °C is 0.43 while it is 0.60 for the one crystallized at 135 °C. Therefore, the decrease in  $\gamma$  content with increasing crystallization temperature (above the maximum in Figure 2) cannot be attributed to incomplete crystallization. Further support of the validity of the maximum in Figure 2 comes from studies of isothermal crystallization kinetics that will be discussed shortly.

The formation of the  $\gamma$  polymorph as a function of the crystallization temperature was also studied for all the polymers listed in Table 2. In this series the concentration of defects is constant and very small, about 0.4 mol %. They are mainly of the 1, 2 head-to-head type, with only a minor stereoisomer content. The molecular weight in this group vary from 102 500 to 439 000 g/mol. Only  $\alpha$  crystals are formed after relatively rapid crystallization of the polymers in this group. For crystallization temperatures between 140 and 155 °C, the samples display a weak reflection at  $2\theta = 20.05^\circ$ , which is characteristic of the  $\gamma$  crystals. X-ray diffractograms are shown in Figure 5 for the polymer M102 K0.42 that was crystallized at 145, 155, and 160 °C. The  $\gamma$  fraction is very small in this series, relative to the values found with the polymers from Table 1. It is about 5% after crystallization at 145 °C and increases to about 8% for crystallization at 155 °C. The  $\gamma$  content is negligible, or zero, after crystallization at 160 °C. The transformation at each of these temperatures was complete. Hence, the variations of the  $\gamma$  content with crystallization temperature cannot be attributed to any effect of the crystals formed during quenching. Thus, a small, but significant, amount of the  $\gamma$  form can even be developed at atmospheric pressure in these highly regularly structured isotactic poly(propylenes), when the crystallization is conducted at sufficiently high temperatures. A small,

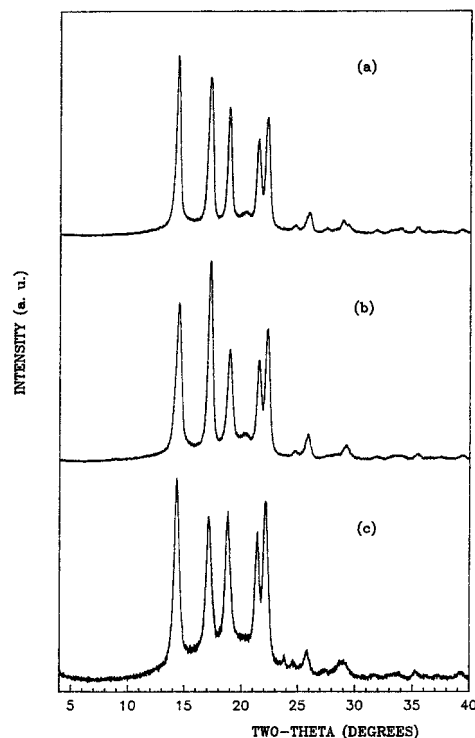


**Figure 5.** WAXS diffractograms of sample M102 K0.42 crystallized at three different temperatures: (a)  $T_c = 145^\circ\text{C}$ , 5%  $\gamma$ ; (b)  $T_c = 155^\circ\text{C}$ , 8%  $\gamma$ ; (c)  $T_c = 160^\circ\text{C}$ , 0%. Note the absence of  $\gamma$  reflection in the sample crystallized at 160 °C.

but discernible, maximum in the fraction of  $\gamma$  form with crystallization temperature is also observed.

**Effect of Varying Defect Concentration.** The above results give an indication that the optimum  $\gamma$  content that can be achieved after isothermal crystallization of homopolymers increases with defect concentration. To examine this effect on a quantitative basis, a series of polymers whose defect content ranged from 0.3% to 2.35%, stereo and regio defects included, were also studied. The polymers in this series are those listed in Table 3. These polymers are not of strictly uniform molecular weight. However, in this range of high molecular weight the effect of chain length on the formation of the  $\gamma$  polymorph is, as noted in the previous section, negligible. The pair of samples M346K 1.00 and M236 K1.17 is of particular interest because they have about the same fractional content of defects but of the reverse type; i.e., M346 K1.00 contains 0.84 mol % stereo defects and 0.16 mol % of 2,1 additions while M236 K1.17 has 0.22 mol % stereo and 0.95 mol % of 2,1 additions. A comparison of the results for this pair will ascertain whether the formation of the  $\gamma$  form is enhanced by a specific defect type. Rapid crystallizations of all of these polymers, such as crystallization in ice water or at 25 °C, led to the formation of only  $\alpha$  crystals.<sup>43</sup>

The results with this series follow the trends that have already been described. For a given polymer the  $\gamma$  form is favored at high crystallization temperatures below the maximum. The temperature at which  $\gamma$  crystals are first observed increases with decreasing concentration of defects. For example, the polymer with the lowest defect concentration, 0.30%, does not show any  $\gamma$  crystals over the whole temperature interval studied. Even after crystallization at temperatures as high as 164 °C, the diffractogram was characteristic of the  $\alpha$  form. If a very small amount of  $\gamma$  was formed, it

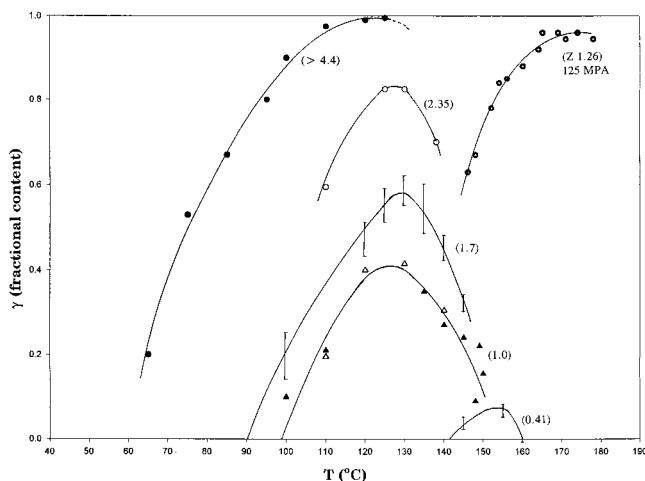


**Figure 6.** Variation of the fraction of the  $\gamma$  polymorph in isotactic poly(propylenes) as a function of percentage of chain defects and crystallization temperature. This work:  $\circ$ ,  $\triangle$ ,  $\blacktriangle$  (the ranges of values indicated as I includes the values of percent  $\gamma$  obtained with different molecular weights (see Figure 3). Literature data:  $\bullet$ , low molecular weight iPP from ref 28;  $\circ$ , Ziegler–Natta iPP crystallized at high pressure from ref 12.

was not resolved. We have found in the previous series that a small  $\gamma$  content can be observed with defect concentrations of about 0.40%. In contrast, the polymer in this series with the highest defect content (2.35%) shows no, or a very small, concentration of  $\gamma$  form at the low crystallization temperatures and very high values, >82%, when crystallized at 124.5 °C. Prolonged crystallization of this sample at 138 °C led to smaller values of the concentration of the  $\gamma$  form (70%) and also confirms the existence of the maximum in this polymer.

Figure 6 is a compilation of the fractional content of  $\gamma$  that forms as a function of the crystallization temperature for the polymers listed in Table 3, as well as the available literature data. Each curve represents the data for a different defect content. The bars in the curves for the polymers with 1.7 and 0.4 mol % defects indicate the range of values obtained with the different molecular weights (Tables 1 and 2). The literature data are those of Thomann et al.<sup>28</sup> for a metallocene isotactic poly(propylene) having a defect concentration greater than 4.4 mol % and that of Phillips et al.<sup>44</sup> for an unfractionated Ziegler-type isotactic poly(propylene), 1.2 mol % defects, crystallized under a pressure of 125 MPa. The quantitative aspects of the figure demonstrate in a dramatic fashion the role of crystallization temperature and defect concentration on the development of the  $\gamma$  form. As an example for crystallization at 100 °C, the  $\gamma$  content is ~0% for polymers with 1 mol % defects; 20% for polymers in Table 1, defect content 1.7 mol %; approximately 45% for polymer M355 K2.35 that has 2.35 mol % defects; and 90% for the low molecular weight polymer studied by Thomann et al.<sup>28</sup> that has a defect content greater than 4.4 mol %. The maximum percentage of  $\gamma$  that is developed follows a similar pattern being 40%, 60%, 83%, and 100% for the respective polymers and only about 8% for the polymer containing 0.40% defects. To develop a  $\gamma$  concentration of 50% at the left side of the maximum requires crystallization at 120 °C for polymers listed in Table 1 (1.70 mol % defects). The polymer having greater than 4.4 mol % defect only requires a 75 °C crystallization temperature to achieve the same value for the  $\gamma$  concentration. This difference in crystallization tem-

perature also shifts the formation of equivalent  $\gamma$  concentrations to higher undercoolings with increasing defect content. These temperatures correspond to undercoolings of 63 and 102 °C when 186 °C is taken as the equilibrium melting temperature,  $T_m^0$ , of the  $\gamma$  form.<sup>45</sup> The undercooling differences would be qualitatively similar if a higher value was taken for  $T_m^0$ .<sup>46,47</sup> This effect of temperature is even more marked at low  $\gamma$  concentrations. For example, a  $\gamma$  content of 5% is achieved at 60 °C for the polymer with greater than 4.4 mol % of defects, while 145 °C is required for the 0.4% sample. This is a dramatic change for forming just a small amount of  $\gamma$ . Thus, the defect content and the crystallization temperature are the key variables that govern the fraction of  $\gamma$  that is formed. Although the role of these two variables has been discussed qualitatively previously,<sup>28</sup> we find in Figure 6 a comprehensive set of detailed quantitative data covering a wide range in defect concentration and crystallization temperatures.

Interestingly, the two polymers with essentially the same total defect content, M346 K1.00 and M236 K1.17, but inversely distributed between stereo and regio develop identical values of the fractional content of the  $\gamma$  form at all crystallization temperatures. The results for this pair are represented in Figure 6 by the open and closed triangles. We can conclude from these results that the two types of defects have the same influence in the formation of the  $\gamma$  polymorph.

The Ziegler–Natta catalyzed polymer that contains 1.26% stereo defects, and no regio ones, behaves in a similar manner when crystallized under pressure. Under atmospheric pressure the  $\gamma$  form cannot be developed over the accessible temperature range for crystallization.<sup>11</sup> However, when crystallized under 125 MPa about 65% of the  $\gamma$  polymorph develops at 145 °C. There is, initially, a continuous increase in the  $\gamma$  content as the crystallization temperature is increased. A maximum, or leveling off, is then reached at the highest temperatures studied. Much higher  $\gamma$  concentration levels are observed than would be expected from the atmospheric pressure studies that have been described. A major consequence of applying hydrostatic pressure is that it enables the crystallization to be conducted at higher temperatures. Thus, for this reason alone higher  $\gamma$  concentrations are expected relative to those obtained at atmospheric pressure. There may also be an influence of the applied pressure on the crystallization kinetics. This in turn could influence the development of the  $\gamma$  form.<sup>48</sup>

The maximum fraction of  $\gamma$  that was obtained for each of the polymers listed in Table 3, as well as one from Table 2 with just regio defects (M182 K0.40), is plotted against the total defect concentration in Figure 7. The bars represent the range of experimental values obtained at temperatures in the vicinity of the maximum. Also indicated with each data point are the regio and stereo fractions of the polymer, the stereo ones preceding the regios. The solid straight line that is drawn is an approximate representation of the data. This straight line extrapolates to  $2.8 \pm 0.1$  as the minimum percentage of defects that will allow 100% crystallization of the  $\gamma$  form at the optimum crystallization temperature. This conclusion is based on the molecular weight range studied. Very low molecular weight polymers may behave in a somewhat different manner for reasons that will be discussed shortly.



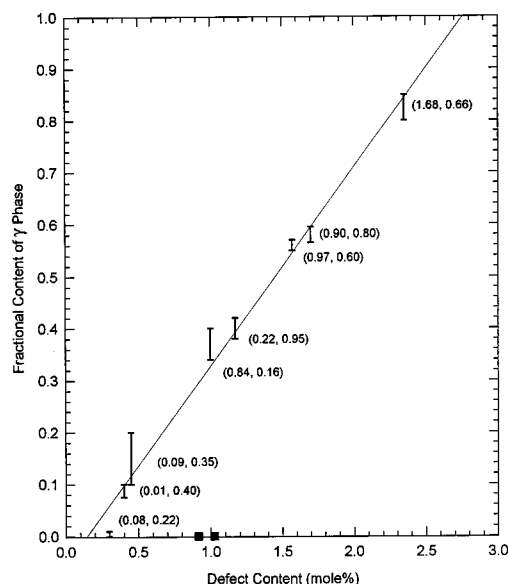


**Figure 7.** Maximum value of the fractional content of  $\gamma$  polymorph as a function of the concentration of chain defects for metallocene poly(propylenes) (I) and commercial Ziegler-Natta type (■). The range of values in I are from samples with different molecular weights as well as from different crystallizations at temperatures in the region of the maximum of Figure 6.

The two Ziegler-Natta catalyzed samples that were studied, which only contain stereo defects, are also included in Figure 7. Sample A, with 0.86% stereo defects, was isothermally crystallized at six different temperatures over the range between 26 and 164 °C. The  $\gamma$  phase was not found under any of these crystallization conditions. Sample B, with 1.02% stereo defects, was crystallized at 26 and 145 °C. As was found with sample A, only the  $\alpha$  polymorph was formed. The polymer studied by Mezghani and Phillips, which contained 1.26 mol % of stereo defects, also did not form the  $\gamma$  polymorph when crystallized at atmospheric pressure.<sup>11</sup> If these Ziegler-Natta type polymers followed the pattern of the metallocenes, then between 25% and 40% of  $\gamma$  form would be expected. It should be noted that the Ziegler-Natta polymers studied by Fischer and Mülhaupt<sup>29</sup> developed about 20% of the  $\gamma$  form. However, the defect concentration of these polymers was not given so that a comparison with the metallocene type isotactic poly(propylenes) cannot be made. Other literature reports indicate only small concentrations of the  $\gamma$  phase in Ziegler-Natta isotactic poly(propylenes).<sup>49</sup> The difference in behavior between the two types of isotactic poly(propylenes) with respect to  $\gamma$  formation must be related to the broad distribution of the defect content of commercial Ziegler type polypropylenes. Thus, although the overall concentration of defects is about 1 mol %, a relatively large number of these defects may be concentrated in a small fraction of poorly crystallizable molecules, which will have a minor contribution to the crystalline properties.<sup>50</sup>

Fischer and Mülhaupt<sup>29</sup> have suggested that the average isotactic segment length  $n_{iso}$ , also termed average meso run length,<sup>50</sup> is an important factor in determining the  $\gamma$  fraction that can be achieved. This postulate is in accord with the observation that higher defect content favors  $\gamma$  formation. Accordingly, the average isotactic segment length, calculated according to eq 1, is plotted in Figure 8 against the maximum percentage of the  $\gamma$  form that was obtained. It is clear

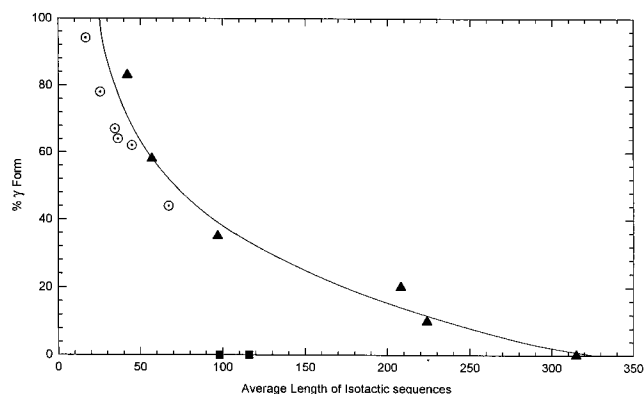


**Figure 8.** Maximum value of the fractional content of the  $\gamma$  polymorph as a function of the average length of isotactic sequences ( $n_{iso}$ ): ▲, metallocenes iPP from this work; ■, Ziegler-Natta iPP from this work; ○, slowly cooled metallocene iPP from ref 29.

that the maximum  $\gamma$  content that can be achieved decreases continuously with average isotactic sequence length. We can estimate from the present work that polymers with  $n_{iso}$  of about 300 units would only produce  $\alpha$  type crystals. In contrast, average sequence lengths of about 35 would yield only the  $\gamma$  form. The values reported by Fischer and Mülhaupt for the  $\gamma$  form of slowly cooled samples (not necessarily the optimum value) are also plotted in Figure 8. To make a comparison with the present work, the reported  $n_{iso}$  values were recalculated according to eq 1. Their results are in good agreement with those obtained in this work, particularly in consideration of the different crystallization methods used. The important conclusion from Figure 8 is that very small sequences of isotactic poly(propylene) can crystallize in the 3/1 helical form and do so as the  $\gamma$  polymorph. On the other hand, with very long sequences, only the  $\alpha$  polymorph forms, while the same ordered conformation is maintained.

The work reported here has been for high molecular weight polymers so that the results are essentially independent of chain length. However, for very low molecular weights that have the same level of defect content, the  $n_{iso}$  values, calculated by eq 1, will be reduced significantly. This explains in a quantitative manner why low molecular weights crystallize predominantly in the  $\gamma$  form.<sup>14-17,28</sup> The crystallization of a low molecular weight of isotactic poly(propylene) allowed for the determination of the crystal structure of the  $\gamma$  polymorph.<sup>6,7</sup>

**Melting.** With the establishment of the conditions for  $\gamma$  formation in terms of the chain microstructure and crystallization temperature, we next examine the fusion behavior. Thermograms of four polymers from Table 1, that were crystallized at four different temperatures, are given in Figure 9. All of the thermograms show multiple endothermic peaks. The thermograms for crystallization at 60 °C are given in Figure 9A. Under these crystallization conditions the WAXS patterns have shown that only the  $\alpha$  polymorph is formed. Two endothermic peaks are observed that have been identified with the two different lamellae types that are associated with the  $\alpha$  form.<sup>3</sup> A mesh, crosshatched type lamellar morphology is observed with these crystals. The low-temperature endotherm represents the melting of thinner transversal lamellae while the higher-temperature endotherm is due to the melting of the radial (usually thicker) lamellae.<sup>3</sup> For relatively low crystal-

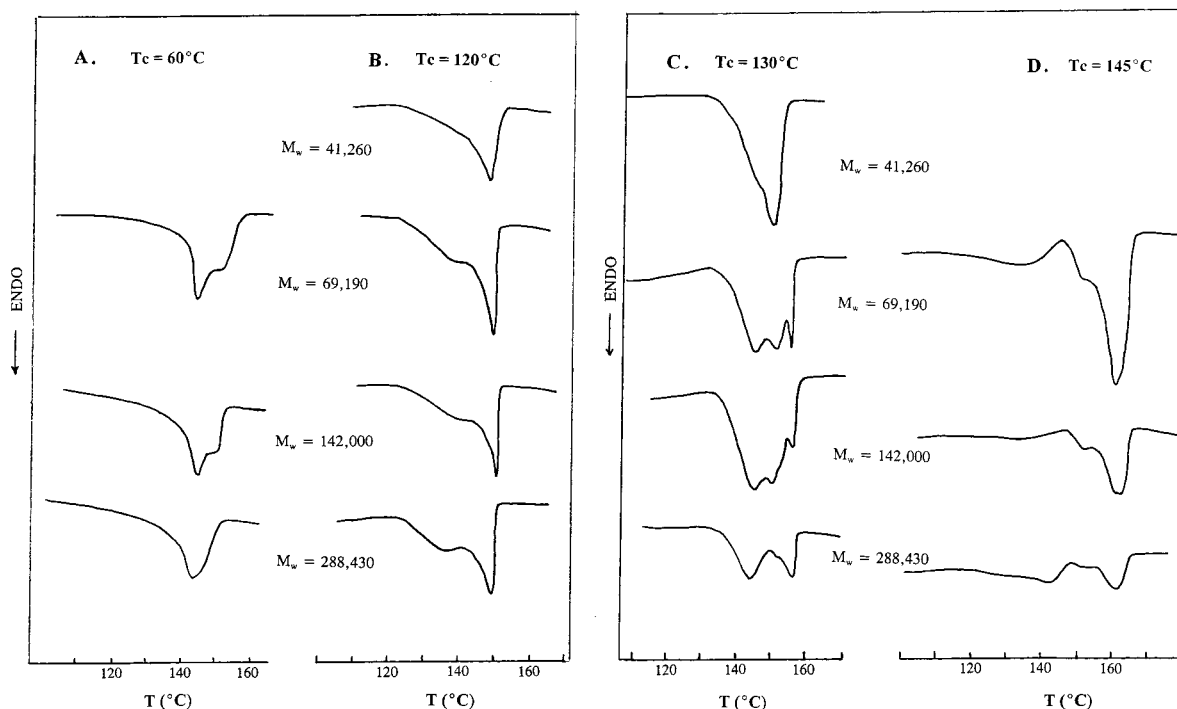


**Figure 9.** DSC endotherms of iPP from Table 1 crystallized at the indicated temperatures. See text for discussion of multiple endotherms.

lization temperatures there could also be a contribution from a melting–recrystallization process.

After crystallization at 120 °C (Figure 9B), a major endothermic peak is observed at 149.5 °C along with a low-temperature shoulder. The shoulder becomes better defined with the higher molecular weight samples. The relative areas of the two peaks are qualitatively similar to the ratio of the  $\gamma$  to  $\alpha$  contents of these samples. It is, therefore, tempting to postulate that the two peaks represent the melting of the  $\alpha$  and  $\gamma$  forms, respectively. This postulate will be addressed after the thermograms for the higher crystallization temperature and the diffractograms obtained during melting are analyzed.

The thermograms in Figure 9C for crystallization at 130 °C, which corresponds to the temperature of the maximum in Figure 2, display some unique features. For polymers with molecular weights between 68 000 and 169 800 g/mol, three separate endothermic peaks are resolved. The central endotherm of the highest molecular weight studied is less intense and overlaps with the high-temperature endotherm. These peaks are not a consequence of a melting followed by recrystallization process because varying the heating rate does not change the number or relative intensity of these peaks. All three peaks develop simultaneously during the initial stages of the crystallization. They could be associated with melting of different morphological or crystallographic entities. Qualitatively similar results are obtained for crystallization temperatures between 125 and 140 °C. No quenching peaks are observed in the thermograms for crystallization temperatures up to 130 °C. The absence of such peaks indicates that at crystallization temperatures equal to, or less than, 130 °C the transformation is complete.

After crystallization at 145 °C for 6 days (Figure 9D), a low-temperature endotherm at about 137 °C is found that is due to the crystallites formed on quenching. Besides this broad quenching peak, the thermograms of the samples show two melting peaks. Thus, it appears

that at the high crystallization temperatures the middle endotherm shifts to higher melting temperatures and overlaps with the high melting peak. The intensity of the low melting peak at  $T_c = 145$  °C decreases considerably with respect to the intensity of the same peak for  $T_c = 130$  °C. As will be demonstrated shortly, the low-temperature peak corresponds to melting of  $\gamma$  type crystals; therefore, the variation of the intensity of this peak with  $T_c$  in Figure 9B–D parallels the variation of the fractional content of  $\gamma$  form shown previously (see Figure 2). The resolution of the three different structures into separate melting endotherms appears to depend on the molecular weight of the polymer. Inspecting Figure 9C,  $T_c = 130$  °C, the lowest molecular weight only gives a broad melting peak, and the central endotherm of the highest molecular weight polymer is only resolved as a broad shoulder. The intermediate molecular weights clearly show the three melting endotherms. The variation of the melting behavior with molecular weight seems to reflect variations of the average crystallite thickness of both polymorphs with molecular weight.

To investigate the origin of the three melting endotherms observed for crystallization temperatures between 125 and 140 °C for the samples listed in Table 1, of which Figure 9C is an example, WAXS and birefringence studies were carried out with sample M142 K1.70 that was isothermally crystallized at 135 °C. A DSC melting thermogram was obtained under the same crystallization conditions. This thermogram serves as a reference to identify the temperatures of interest in the diffractograms and is given as an insert to Figure 10. Wide-angle X-ray scattering patterns were obtained at a series of temperatures that were dictated by the main features of the thermogram. These patterns comprise the main portion of Figure 10. The uppermost diffractogram was taken at 137 °C, which represents a temperature below the melting range. Thus, the fractions of the  $\alpha$  and  $\gamma$  form obtained at this temperature



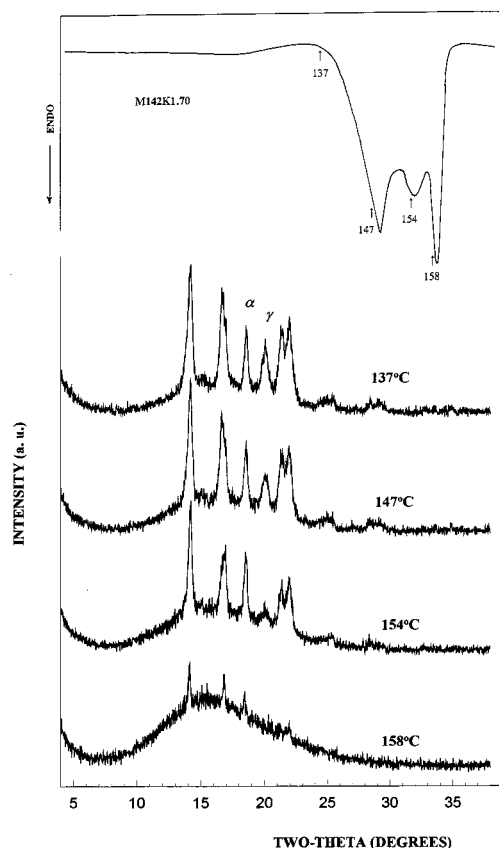


**Figure 10.** Top: DSC melting thermogram of sample M142K1.70 crystallized at 135 °C. Lower: WAXS diffractograms of the same sample obtained at the temperatures indicated by arrows in the thermogram. The relative variations of the  $\alpha$  or  $\gamma$  reflections with temperature are discussed in the text.

are the same as those at room temperature. As the temperature is raised to 147 °C, close to the peak of the lowest endotherm, the 117 reflection, characteristic of the  $\gamma$  polymorph, decreases significantly. However, the intensity and width of the characteristic  $\alpha$  reflection remain constant. It is clear, therefore, that the  $\gamma$  polymorph begins to melt at a temperature lower than that for the  $\alpha$  form. At 154 °C, the temperature which corresponds to the peak of the central endotherm, the  $\gamma$  polymorph is still observed in the diffractogram, although its content has decreased to less than 10%. In contrast, at this temperature the intensity and width of the  $\alpha$  reflection remained constant. Thus, the diffractogram recorded in the temperature region of the two lowest endotherms shows that the  $\gamma$  polymorph has preferentially melted. There is no contribution from the  $\alpha$  crystal to these two endotherms. Only in the temperature region of 158 °C, which corresponds to the sharp, highest temperature endotherm, does the characteristic 130 reflection of the  $\alpha$  form decrease and eventually vanish. The two melting endotherms attributed to the  $\gamma$  polymorph could be caused by either two crystallite populations with different average thicknesses or two sets of crystallites with similar thicknesses but having different morphologies. The possible  $\gamma$  structures will be discussed shortly.

Unusual lamellar morphologies were observed for  $\gamma$  isotactic poly(propylene) spherulites formed at elevated pressure.<sup>12</sup> Radial lamellar patches, postulated to be either the  $\alpha$  or  $\gamma$  phase, were reported to melt at temperatures  $\sim 10$  °C lower than featherlike structures

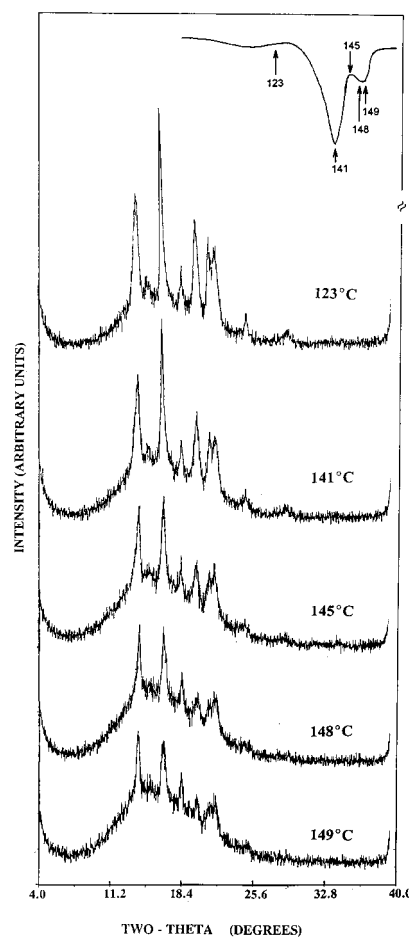


**Figure 11.** DSC melting and WAXS diffractograms at different temperatures during melting for sample M335K2.35 crystallized at 124.5 °C. The temperatures at which WAXS were obtained are indicated by arrows in the thermogram.

grown epitaxially. In our studies of crystallization at atmospheric pressure the  $\alpha$  phase has never shown to have a lower melting temperature than the  $\gamma$  phase. Thus, if thin lamellae are part of the morphology of  $\gamma$  crystals formed at high pressure, by analogy with our studies, they most probably are of the  $\gamma$  form. We have investigated this hypothesis further by studying the crystallization and melting of both crystallographic forms in our poly(propylene) sample that had the highest  $\gamma$  content. The WAXS studies were again correlated with thermal measurements. Figure 11 depicts the DSC thermograms and WAXS patterns of polymer M335 K2.35 that was crystallized at 124.5 °C for 4 days. The  $\gamma$  content of this sample is 82.5%. The WAXS patterns were obtained at room temperature and at the temperatures indicated by the arrows in the thermogram. Paralleling the results shown in Figure 10, for a polymer that contained a lower defect content, the intensity of the 130 reflection ( $2\theta = 18.8^\circ$ ), which identifies the  $\alpha$  crystals, remains constant until the final stages of melting. At temperatures that correspond to the intense high-temperature endotherm and its vicinity, 148 and 149 °C, the intensity of the  $\gamma$  peak at  $2\theta = 20.05^\circ$  decreases significantly, but it does not completely vanish. The two last diffractograms show that a small percentage of  $\gamma$  crystals remain even at temperatures close to complete melting. Thus, the association of the low-temperature peak with the complete melting of the  $\gamma$  crystals, and the high-temperature one with the melting of  $\alpha$ , is not completely supported by the results

shown in Figures 10 and 11. Although only  $\gamma$  crystallites contribute to the low melting endotherm and the melting of all of  $\alpha$  is reflected in the high-temperature endotherm, a small concentration of  $\gamma$  crystals, a few percent, melt in the temperature region of the high melting peak. The melting of this second population of  $\gamma$  crystals was resolved as a distinct endotherm in Figure 10 for a sample with fewer defects. However, it does not show as a third endotherm in Figure 11 when a higher content of  $\gamma$  phase is involved. This middle endotherm is most probably buried within the high-temperature endotherm.

The results shown in Figures 10 and 11 indicate that the  $\gamma$  reflection is observed within both the low- and high-temperature endotherms, albeit with quite different intensities. On the basis of these results, two different morphological  $\gamma$  structures can be postulated to coexist with the  $\alpha$  form. It has also been concluded, on the basis of microscopic observations, that the  $\gamma$  crystals exist in two different morphological forms.<sup>12,28</sup> The atomic force microscopic studies of Thomann et al.<sup>28</sup> clearly distinguished bundlelike entities of the  $\gamma$  phase growing as triangular slices arranged in rows in an angle of  $80^\circ$  to each other on  $\alpha$  structures. These entities exist along with structures of pure  $\gamma$  entities. The present thermodynamic and WAXS results strongly support the conclusion drawn from the microscopic studies. An explanation for the existence of three different lamellar entities, with distinctly different melting behavior, can be given on the basis of crystallographic modes of lamellar packing for the  $\alpha$  and  $\gamma$  polymorphs.<sup>1,51</sup> These models favor epitaxial crystallization of  $\alpha$  from  $\alpha$  and of  $\gamma$  from  $\alpha$  forms and, thus, support the common observation of the  $\alpha$ - $\alpha$  and  $\alpha$ - $\gamma$  branching. However, they do not allow for  $\gamma$ - $\gamma$  branching. Although speculative at this stage, it is not unreasonable to associate the low-temperature peak with unbranched  $\gamma$  crystals and the middle peak with melting of  $\gamma$  crystals that grew epitaxially on a preexisting  $\alpha$  surface. The relative percentage of the latter crystals that are formed is conditional to the percentage of  $\alpha$  crystals formed in the high-temperature region in which the  $\gamma$  phase develops. This explains the lack of resolution of a distinct middle endotherm in Figure 11 since the percentage of crystals of the  $\alpha$  polymorph in this sample is only 17%. The validity and details of these possibilities representing the two different  $\gamma$  morphologies still need to be elucidated.

The relation between the polymorphic form developed at a given temperature and its melting behavior was also studied by optical microscopy. As an example, it was found that the sign of the birefringence of the spherulites of sample M142K1.70, crystallized at  $135^\circ\text{C}$  whose melting was depicted in Figure 10, is preferentially positive. This positive birefringence is due primarily to the  $\sim 55\%$  of  $\gamma$  crystals present and perhaps also by some daughter, transversal,  $\alpha$  type lamellae. The sign changes to a mixed-type birefringence at a temperature corresponding to the lowest temperature endotherm ( $148^\circ\text{C}$ ). This change is in agreement with partial melting of the  $\gamma$  crystals. At  $154^\circ\text{C}$ , the temperature corresponding to the peak of the middle endotherm shown in Figure 10, the WAXS diffractogram indicates that a small fraction of  $\gamma$  crystals still remain together with all of the  $\alpha$  ones. However, the sign of the birefringence changes to negative at this temperature. This change confirms that the  $\alpha$  type lamellar crystals

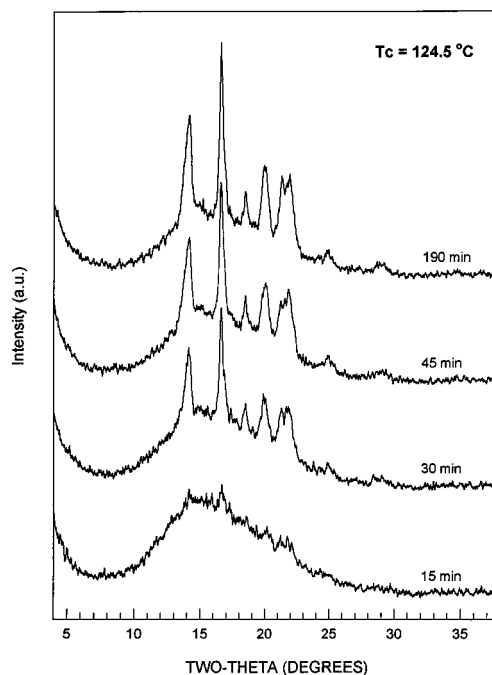


**Figure 12.** WAXS diffractograms of sample M335K2.35 crystallized at  $124.5^\circ\text{C}$  as a function of crystallization time. Both polymorphs form from the early stages of the crystallization.

are relatively long and radially oriented, conferring this negative character to the global birefringence of the spherulites. These crystallites melt sharply at about  $160^\circ\text{C}$ , in agreement with the highest temperature peak in the thermogram.

**Kinetics.** Studies of the crystallization kinetics from the melt of the two polymorphs should contribute to our understanding of the mechanisms involved in their formation. Consequently, we undertook such studies using WAXS and DSC techniques. The total fusion process is characterized by a low-melting endotherm that is characteristic of the melting of the  $\gamma$  crystallites and a high-temperature one that corresponds primarily to the  $\alpha$  form. Thus, by monitoring the development of each of the endothermic peaks as a function of time, and converting them to heats of fusion, a quantitative kinetic analysis can be made that complements the WAXS studies.

Wide-angle X-ray scattering patterns were obtained in situ of the crystallization of M335K2.35 at  $124.5^\circ\text{C}$  as a function of time. This polymer has the highest defect content among the isotactic poly(propylenes) that were studied here. The results are given in Figure 12 for the indicated crystallization times. Both polymorphs are observed at the very onset of the crystallization as is indicated by the pattern obtained after crystallization for 15 min. In the early steps of the crystallization the relative intensities of the two reflections, characteristic of each polymorph, remain essentially constant. However, after 45 min the reflection characteristic of the  $\gamma$  form increases continuously, while that of the  $\alpha$  does not change.

The thermograms for the same polymer, crystallized at the same temperature,  $124.5^\circ\text{C}$ , without further cooling, are shown in Figure 13. Two endotherms are observed at the very early stages of the crystallization, and they increase in parallel up to a crystallization time of 65 min. At longer times the intensity of the higher temperature peak remains constant while that of the

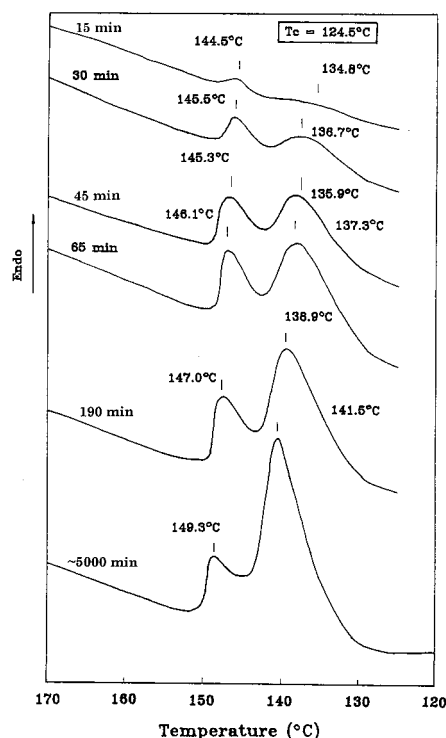


**Figure 13.** DSC melting endotherms of sample M335K2.35 crystallized at 124.5 °C as a function of crystallization time. Melting after crystallization up to 190 min was started from the crystallization temperature, without previous cooling. The lowest endotherm was obtained in a sample crystallized in an oil bath. Thus, the melting process was started at 37 °C. (Note that in this plot the melting peaks are displayed facing upward, opposite to meltings shown in Figures 2 and 9.)

low-melting peak continues to increase. From the thermograms about 80% of the  $\gamma$  form develops at this crystallization temperature as compared to 83% after complete transformation as determined by WAXS. A comparison of the diffractograms with the thermograms (Figures 12 and 13) demonstrates that as the crystallization progresses, the relative intensities of the reflections that correspond to each of the polymorphs correlate very well with the enthalpies of fusion obtained from the two endotherms, and thus the two crystalline forms.

The crystallization kinetics of this polymer were also studied at temperatures between 117 and 138 °C. The results are summarized in Figure 14. Here the degrees of crystallinity of each of the forms,  $(1 - \lambda)_{\Delta H}$ , obtained from the enthalpies of fusion, are plotted against log time for each crystallization temperature.<sup>52</sup> Sigmoidal-type isotherms, which are typical of crystallizing polymers, are obtained for both polymorphs. The time scale that ranges from several minutes to several thousand minutes is indicative of a nucleation-controlled process.<sup>53</sup> A major conclusion from these results, made quite clear in Figure 14, is that the crystallization of both polymorphs begins at the same time, at any given temperature. At the very initial stages of the crystallization, the crystallization rates are the same for both polymorphs. A similar conclusion was reached from analysis of the WAXS patterns. However, as the crystallization progresses at constant temperature, the  $\alpha$  crystallinity becomes constant. Eventually, the concentrations of  $\gamma$  crystals given in Figure 6 for the crystalline region are reached. The crystallization kinetics of polymer M346 K1.00 (not shown), with 1 mol % of chain

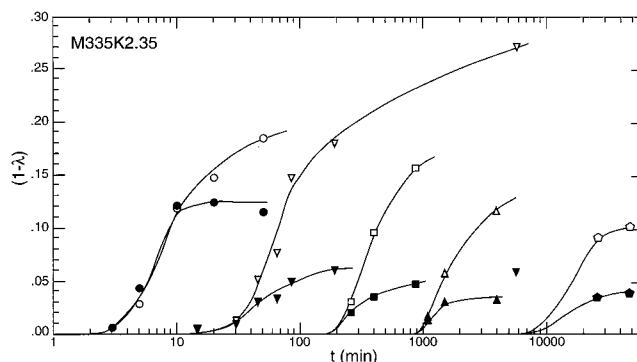


**Figure 14.** Sigmoidal variation of the development of  $\alpha$  and  $\gamma$  crystallinities,  $(1 - \lambda)$ , with time for sample M335K2.35 crystallized at the following temperatures: (○, ●) 117 °C, (▽, ▼) 124.5 °C, (□, ■) 129 °C, (△, ▲) 133 °C, (◇, ◆) 138 °C. Open symbols,  $\gamma$  crystallinity; closed symbols,  $\alpha$  crystallinity.

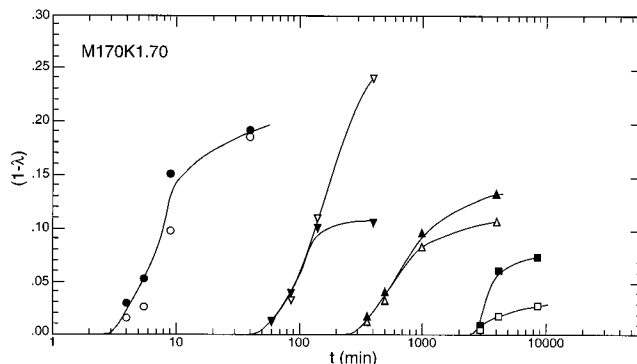


**Figure 15.** Sigmoidal variation of the development of  $\alpha$  and  $\gamma$  crystallinities,  $(1 - \lambda)$ , with time for sample M170K1.70 crystallized at the indicated temperatures: (○, ●) 120 °C, (▽, ▼) 130 °C, (△, ▲) 136 °C, (□, ■) 140 °C. Open symbols,  $\gamma$  crystallinity; closed symbols,  $\alpha$  crystallinity.

defects, shows some similar as well as some significantly different characteristics. The crystallization of both polymorphs is again initiated at the same time, and the initial crystallization rates are also the same. In contrast with the results in Figure 14, however, it is the  $\gamma$  content that now levels off and becomes constant, while the  $\alpha$  content continues to increase with time to satisfy the higher fractional content of  $\alpha$  formed at any temperature (Figure 6). Thus, this aspect of the crystallization process is just the opposite from that for the polymer that contains 2.35 mol % of defects. The reason for this behavior resides in the difference in defect concentrations between the two polymers and, thus, the final relative  $\gamma$  content (~40% of the crystals) that this polymer develops.

The crystallization kinetics of polymer M107 K1.70 were also studied at temperatures between 120 and 140 °C. The results are given in Figure 15 for four different crystallization temperatures:  $T_c = 120$  °C, below the maximum;  $T_c = 130$  °C, the maximum temperature; and  $T_c = 136$  and 140 °C, above the maximum. The defect concentration of this polymer is intermediate between that of the two polymers just discussed. The initial crystallization times and rates of the two polymorphs are again found to be the same at each crystallization temperature. This behavior thus appears to be universal for the crystallization of the polymorphs in isotactic poly(propylene). At 120 °C, both polymorphs crystallize very rapidly and at about the same rate over the entire transformation. At 130 °C, although the crystallization rates for both forms are virtually identical at the early



stages of the crystallization, the concentration of the  $\alpha$  crystals formed from the melt levels off at relative early times, while the  $\gamma$  continue to crystallize. Thus, increasing the temperature enhances the material transformed to  $\gamma$ . However, at the right side of the maximum, 136 and 140 °C, the situation is reversed. The  $\gamma$  content levels off to a relatively low concentration, while the  $\alpha$  crystallizes to a significantly higher level. The kinetic data of Figure 15 give further and direct substantiation of the maximum observed in Figure 6 for the polymers of Table 1. We can also conclude from these kinetic studies that the initial crystallization rate from the melt is the same for both polymorphs.

The heat of fusion for each of the polymorphs, as well as the total, is plotted in parts a and c of Figure 16 for M107 K1.70 and M335 K2.35, respectively. The total degree of crystallinity ranges from about 0.40 at 120 °C to about 0.14 at 140 °C. The fractional content obtained for each polymorph at a given temperature can be calculated from these data. The heat of fusion at any given temperature is taken as the value corresponding to 1 decade of time in the flat portion of the isotherm. The independent variation of the heat of fusion at the final stages of the transformation for the  $\alpha$  and the  $\gamma$  polymorphs gives the variation with temperature of the contents of  $\alpha$  and  $\gamma$  crystals formed from the original melt, i.e., the variation of the  $\alpha$  crystallinity and  $\gamma$  crystallinity. While the variation of the  $\alpha$  crystallinity follows the expected trend that has been observed with other random copolymers,<sup>54,55</sup> the variation of the  $\gamma$  crystallinity with temperature goes through a maximum, reflecting again that two competing mechanisms are involved in the formation of this polymorph. The ultimate fraction of  $\gamma$  crystals that is obtained at each crystallization temperature is plotted in Figure 16b,d for each polymer. Very good agreement is obtained between the WAXS and DSC data for the fractional content of the  $\gamma$  polymorph in the crystalline region. Consistent with the WAXS results shown in Figure 6, the fractional content of  $\gamma$  calculated from heat of fusion also shows a maximum in the same temperature region (Figure 16b,d). These data indicate that, in the interval of molecular weights studied here, the relative contents of the  $\alpha$  and  $\gamma$  polymorphs in isotactic poly(propylenes) can be estimated from the analysis of the heat of fusion of the respective melting peaks.

### Summary and Discussion

The crystal structure (unit cell) of the  $\gamma$  polymorph and the condition for its formation bring some special features to the study of polymer crystallization. The unit cell of this form is unique among polymer crystal structures in that the chains are not parallel to one another.<sup>6,7</sup> The conditions for forming this polymorph are also unusual as it depends in a very specific way on both the chain microstructure and the crystallization temperature. A full understanding of the formation of  $\gamma$  and its structure involves correlating these apparently diverse facts.

Central to all considerations is the role of the chain microstructure. Figure 6 makes clear that as the defect (regio and stereo) concentration increases, the propensity for  $\gamma$  formation is enhanced. One only needs to compare the results for the polymer studied by Thomann et al.<sup>28</sup> with the one studied here, which contains 0.40% regio defects. In the former case, the polymer has a defect concentration greater than 4.4%, and 100% of

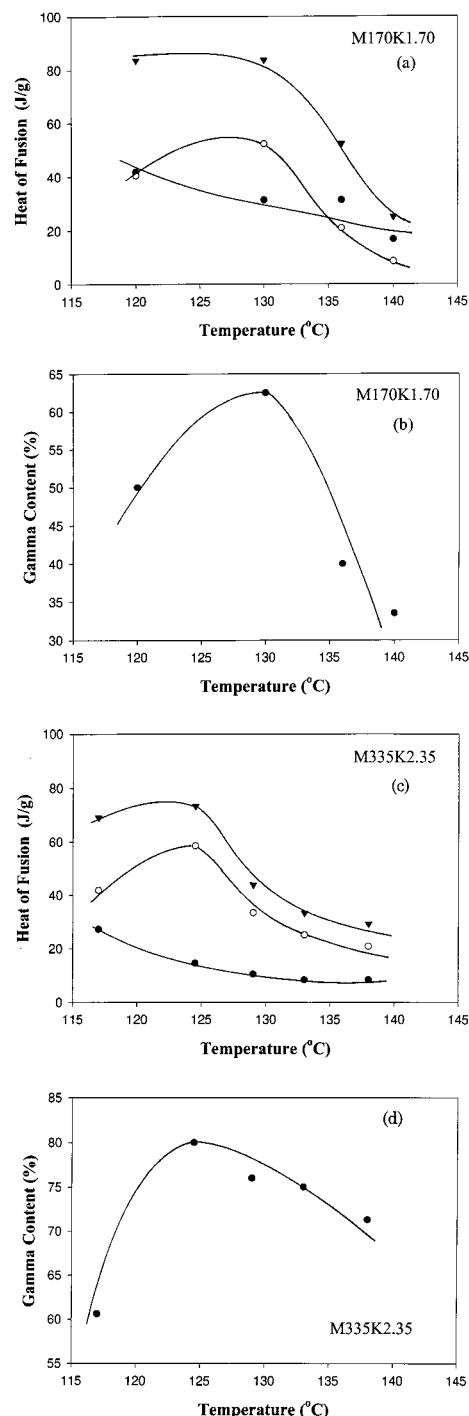


**Figure 16.** (a, c) Variation of the independent heat of fusion of  $\alpha$  type crystals (●) and  $\gamma$  crystals (○) as well as the combined heat of fusion as a function of crystallization temperature. The heats of fusion at a given temperature were taken as the value corresponding to 1 decade of time in the flat portion of the isotherm. (a) Sample M170K1.70, (c) sample M335K2.35. (b, d) Variation with crystallization temperature of the calculated percentage of  $\gamma$  form from the data in (a) and (c).

the  $\gamma$  structure could be developed. In the latter case, the maximum  $\gamma$  concentration that can be formed is 10% at best. Extrapolation of these results indicates that only very small amounts, if any, of the  $\gamma$  form would develop in the pure polymer devoid of any defects. In fact, Thomann et al.<sup>28</sup> report that only the  $\alpha$  polymorph could be formed in a sample of isotactic poly(propylene) of  $M = 16\,000$  g/mol that was devoid of any type of irregularities in the chain.

The experimental requirement for a significant concentration of chain defects, with the concomitant small average isotactic sequence length between defects, to form an appreciable amount of  $\gamma$  results in crystallites whose dimensions in the chain direction (thickness) will by necessity be small. Thus, only a relatively *small* number of chain units participate in a given  $\gamma$  crystallite. Thomann et al.<sup>28</sup> have estimated that approximately 20 monomer units arranged in a  $3_1$  helix participate in a 40 Å thick lamellae. The development of lamellar crystallites is thermodynamically favored. Electron microscopy studies clearly indicate that one of the  $\gamma$  morphological forms is lamellar-like.<sup>28</sup> However, for a lamellar structure to evolve, the large flux of chains that emanates from the very small crystallite needs to be dissipated.<sup>56</sup> Chain folding, of one type or another, is one common method by which flux in many crystalline chain molecules is dissipated, including the  $\alpha$  form of isotactic poly(propylene). However, this is not a tenable option with extended chains of small isotactic sequences. The very long sequence length of the attached noncrystallizable units precludes any significant folding with adjacent reentry and probably any significant chain folding at all. However, there is another way by which the chain flux can be dissipated, so that crystallization can proceed with the development of lamellar crystallites. This involves tilting of the ordered sequences within the crystallite. For example, in polyethylene the chain flux is reduced by folding (with only a small amount of regular folding randomly distributed along the basal plane) and a modest amount of chain tilting.<sup>57,58</sup> In the situation under consideration here chain tilting is highly favored since the  $\gamma$  crystalline form, with a particular set of tilted chains in the unit cell, represents a low-energy structure.<sup>1,7</sup> The fact that it is crystalline indicates that it represents a low-energy form. Thus, the formation of the ordered  $\gamma$  structure, with the antiparallel tilted chains, is a natural consequence of reducing the flux of chains that emanate from the 001 plane and accommodating chain defects outside the crystal. It has been postulated, without detail, that the features of the crystal-liquid interphase play a significant role in the formation of  $\gamma$ .<sup>59</sup> Other copolymers that have similar sequence distribution, i.e., random ethylene copolymers with a relatively high comonomer content, do not have the advantage of the accessibility of a low-energy three-dimensional ordered structure by chain tilting. Hence, in these cases after a relatively low comonomer content, 3–4%, is added, the crystallites are not longer lamellar, although crystallization occurs.<sup>60,61</sup> There is, therefore, a fundamental reason that the formation of the  $\gamma$  polymorph is so highly favored by isotactic poly(propylene) chains with high concentrations of structural and chemical irregularities, regio units, stereoisomers, and comonomers. These structural irregularities generate short crystallizable sequences, and associated long sequences of noncrystalline units, that are required to form  $\gamma$ . From these considerations it is concluded that the thickness of  $\gamma$  crystals will be restricted and relatively small when compared to the other crystal structures of isotactic poly(propylene), as well as those in other polymers.

Another unique situation exists when one wants to compare the true thermodynamic stability of the  $\gamma$  form with other structures, such as the  $\alpha$ . Conventionally, the thermodynamic properties, particularly the melting temperatures, of very large crystals that are devoid of

surface effects are compared for the different structures. Since large, thick  $\gamma$  crystals cannot be obtained, one is presented with a serious dilemma. Since the properties of only very small  $\gamma$  crystallites can be measured, and even then over a very small and restricted thickness range, extrapolation of melting temperatures, enthalpy, and entropy of fusion to large sizes, including an infinitely thick crystallite, involves very large errors. Pragmatically, therefore, a comparison of the thermodynamic stability of the  $\alpha$  and  $\gamma$  forms can only be made with crystallites that have the same, small thickness. Such samples have not as yet been prepared. Even if this procedure could be followed, there is concern for the contribution of the interfacial free energies associated with the basal planes of each polymorph to the free energies of fusion. With respect to the interphase, chain folding will be minimal with the  $\gamma$  crystallite while the folding that is required in order to propagate an  $\alpha$  type lamellar crystallite will involve an expenditure of free energy.<sup>62,63</sup>

An estimate can be made, however, of the relative stability of the  $\alpha$  and  $\gamma$  forms. For polymers, in general, the major contribution to the entropy of fusion is the conformational change that occurs on melting.<sup>64</sup> Since the ordered chain conformation is the same for both the  $\alpha$  and  $\gamma$  crystals, and the same melt is involved, the entropy of fusion of the two polymorphs should be close to one another. Calculations of the packing energies indicate that the  $\gamma$  form would be slightly more stable than the  $\alpha$ .<sup>1,65</sup> On the basis of these considerations, one can hypothesize that, for the relatively thin crystallites of interest, the  $\gamma$  form will be slightly more stable than the  $\alpha$  one. In the fusion processes that have been described here the low-temperature endotherm was identified with the melting of the  $\gamma$  form. This is a consequence of the very small thickness of the  $\gamma$  as compared to the  $\alpha$ .

A qualitative explanation of the fraction  $\gamma$  that is formed as a function of temperature, as is illustrated in Figure 6, can now be offered. It is based on the chain microstructure requirements with temperature. The salient features that need to be explained are the increase in the relative  $\gamma$  concentration as the crystallization temperature is raised initially, the attainment of a temperature where the maximum  $\gamma$  content is reached, and its subsequent decrease with a further increase in temperature. The presence of the maximum requires that at least two competing mechanisms are involved, each with a different temperature coefficient. The temperatures are considered to be relative to the equilibrium melting temperature and thus to the defect concentration. Treating the defected chain as a random copolymer establishes the sequence distribution. It is also important to recognize the broad melting range typical of random copolymers.<sup>55</sup>

Central to the problem is the question of how the concentration of crystallizable sequences, i.e., those of length that equal or exceed the requirement for a nucleus of critical size, will change with temperature.<sup>54,66</sup> Attention is focused on the dimensions of the critical nucleus since nucleation is the primary step in the crystallization. This quantity can be calculated for the coherent unimolecular deposition on a preexisting substrate.<sup>54</sup> The result of such a calculation is illustrated in Figure 17. Here,  $\xi^*$ , the critical number of repeating units in a chain direction, is plotted against the mole percent of structural irregularities for different

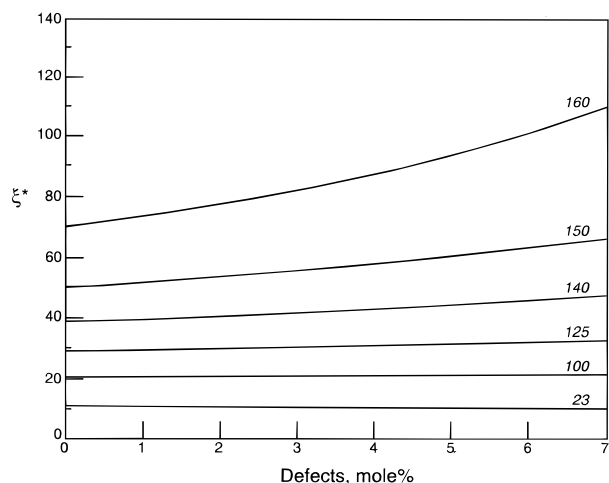


**Figure 17.** Variation of the calculated critical nucleus thickness<sup>54</sup> as a function of the concentration of chain defects of iPP for the indicated crystallization temperatures. In the calculation of  $\xi^*$  a coherent Gibbs type nucleus was adapted with the following parameters:  $\sigma_e = 81.5$  erg/cm<sup>2</sup>,  $\Delta H_u = 19.76 \times 10^8$  erg/cm<sup>3</sup>,  $T_m^0 = 458$  K and infinite molecular weight chain.

crystallization temperatures. This particular calculation was performed with  $\sigma_{en} = 4000$  cal/mol (81.5 erg/cm<sup>2</sup>) and  $T_m^0 = 185$  °C.<sup>67</sup> However, the most important factor is the change in  $\xi^*$  with temperature and composition. From the data in Figure 17 we take as an example the 2.3 mol % defected polymer (M335 K2.35). For this polymer, crystallized at 80 °C, isotactic sequences of 16 repeating units and greater are allowed to participate in the crystallization. With such a small lower limit for  $\xi^*$ , the smaller sequences can crystallize in extended form and the larger ones can fold. Consequently, close to the optimum level of crystallinity is attained. Under these circumstances there is not a sufficient concentration of long noncrystallizable sequences to serve as the "triggering" mechanism to cause formation of  $\gamma$  crystals. Thus, only  $\alpha$  type crystals will be observed. As the crystallization temperature is raised, the  $\xi^*$  requirement increases so that the very short sequences can no longer crystallize. In the remaining grouping of crystallizable sequences the shorter ones can still not crystallize by folding because the associated noncrystallizable sequences have become too long. Thus, in order for a lamellar crystallite to evolve in extended form, from this sequence, tilting and  $\gamma$  formation will occur. As is indicated in Figure 6, as the crystallization temperature is initially increased, the concentration of  $\gamma$  does in fact increase. However, by the same token, as temperature increases, the availability of short sequences for crystallization is being continuously reduced. Thus, there are two competing mechanisms that eventually lead to the maximum in Figure 6. At sufficiently high temperatures, above the maximum, only a small amount, if any, of  $\gamma$  will form due to the higher requirement. Under these circumstances, the noncrystallizability of the shorter sequences that are required will prevent its formation. However, since the  $\alpha$  form only crystallizes from the longer sequences and the lamellar crystallites are propagated by some type of chain folding, they will dominate at the higher crystallization temperature. A similar description can be given to the data plotted in Figure 6 for the other polymers. These arguments are consistent with the kinetic studies that were given in Figures 14–16 and with the details of the lamellar structure. Electron micrographs of sample M335 K2.35

crystallized at 124.5 °C are also in agreement with this discussion.<sup>68</sup> The crystals developed in this sample are 83%  $\gamma$  and 17%  $\alpha$ . The thin section electron micrographs show an asymmetric bimodal population of crystallite thickness with relative contents similar to the fractional content of  $\gamma$  and  $\alpha$  crystals obtained by WAXS. The lamellar thickness of the major population of crystals is 60 Å. This value agrees closely with the calculated value from the average length of isotactic sequences in this sample, 69 Å. In calculating this value, the length of the repeating unit in the  $c$  axis (2.17 Å) and the 40° tilt in  $\gamma$  type crystals of the chain axis with the crystal surface are considered. The thickness of the minor population of lamellae averages 110 Å.

In summary, in a consistent, but qualitative, manner the unique features of the  $\gamma$  polymorph of isotactic polypropylene can be explained. The explanation is based on the confluence of some basic principles. The key factors are the requirement of chains whose microstructure leads to thin crystallites and the structure of the interfacial region that requires tilted ordered chains in order for a lamellar crystallite habit to develop.

**Acknowledgment.** This work was supported by the National Science Foundation Polymer Program (DMR-94-19508) whose aid is gratefully acknowledged. R.G.A. acknowledges support from the Exxon Education Foundation, and M.J.G. acknowledges support from the National Research Council of Argentina (CONICET). We also thank Dr. Eric Lochner of the Materials Research and Technology Center of Florida State University (MARTECH) for helpful discussions.

## References and Notes

- Brückner, S.; Meille, S. V.; Petraccone, V.; Pirozzi, B. *Prog. Polym. Sci.* **1991**, *16*, 361.
- Padden, F. J.; Keith, H. D. *J. Appl. Phys.* **1959**, *30*, 1479.
- Alamo, R. G.; Brown, G.; Mandelkern, L. *Polymer*, in press.
- Addink, E. J.; Beintema, J. *Polymer* **1961**, *2*, 185.
- Turner-Jones, A.; Aizlewood, J. M.; Beckett, D. R. *Makromol. Chem.* **1964**, *75*, 134.
- Brückner, S.; Meille, S. V. *Nature* **1989**, *340*, 455.
- Meille, S. V.; Brückner, S.; Porzio, W. *Macromolecules* **1990**, *23*, 4114.
- Lotz, B.; Graff, S.; Straupé, S.; Wittmann, J. C. *Polymer* **1991**, *32*, 2902.
- Kardos, J. L.; Christiansen, A. W.; Baer, E. *J. Polym. Sci. (A-2)* **1966**, *4*, 777.
- Pae, K. D.; Sauer, J. A.; Morrow, D. R. *Nature* **1966**, *211*, 514.
- Campbell, R. A.; Phillips, P. J.; Lin, J. S. *Polymer* **1993**, *34*, 4809.
- Mezghani, K.; Phillips, P. J. *Polymer* **1997**, *38*, 5725.
- Brückner, S.; Phillips, P. J.; Mezghani, K.; Meille, S. V. *Macromol. Rapid Commun.* **1997**, *18*, 1.
- Lotz, B.; Graff, S.; Wittman, J. C. *J. Polym. Sci., Polym. Phys. Ed.* **1986**, *24*, 2017.
- Morrow, D. R.; Newman, B. A. *J. Appl. Phys.* **1968**, *39*, 4944.
- Kojima, M. *J. Polym. Sci. (B)* **1967**, *5*, 245.
- Kojima, M. *J. Polym. Sci. (A-2)* **1968**, *6*, 1255.
- Turner-Jones, A. *Polymer* **1971**, *12*, 487.
- Mezghani, K.; Phillips, P. J. *Polymer* **1995**, *36*, 2407.
- Cham, P. M.; Marand, H. *ACS Polym. Mater. Sci. Eng.* **1992**, *67*, 365.
- Giuidetti, G. P.; Busi, P.; Ginlianeli, I.; Zannetti, R. *Eur. Polym. J.* **1983**, *19*, 757.
- Horton, A. D. *Trends Polym. Sci.* **1994**, *2*, 158.
- Paukkeri, R.; Väänänen, T.; Lehtinen, A. *Polymer* **1993**, *34*, 2488.
- Lehtinen, A.; Paukkeri, R. *Macromol. Chem. Phys.* **1994**, *195*, 1539.
- Paukkeri, R.; Lehtinen, A. *Polymer* **1994**, *35*, 1673.
- Rieger, B.; Chien, J. C. W. *Polym. Bull.* **1989**, *21*, 159.
- Rieger, B.; Mu, X.; Mallin, D. T.; Ransch, M. D.; Chien, J. C. W. *Macromolecules* **1990**, *23*, 3559.



- (28) Thomann, R.; Wang, C.; Kressler, J.; Mülhaupt, R. *Macromolecules* **1996**, *29*, 8425.
- (29) (a) Fischer, D.; Mülhaupt, R. *Macromol. Chem. Phys.* **1994**, *195*, 1433. (b) Pérez, E.; Zucchi, D.; Sacchi, M. C.; Forlini, F.; Bello, A. *Polymer* **1998**, *40*, 675.
- (30) Marigo, A.; Marega, C.; Zannetti, R.; Paganetto, G.; Canossa, E.; Coletta, F.; Gottardi, F. *Makromol. Chem.* **1989**, *190*, 2805.
- (31) Randall, J. C. *J. Polym. Sci., Polym. Phys. Ed.* **1976**, *14*, 2083.
- (32) Zambelli, A.; Zetta, L.; Sacchi, C.; Wolfsgruber, C. *Macromolecules* **1972**, *5*, 440.
- (33) Grassi, A.; Zambelli, A.; Resconi, L.; Albizzati, E.; Mazzochi, R. *Macromolecules* **1988**, *21*, 617.
- (34) Tsutsui, T.; Mizuno, A.; Kashiwa, N. *Makromol. Chem.* **1989**, *190*, 1177.
- (35) Toyota, A.; Tsutsui, T.; Kashiwa, N. *J. Mol. Catal.* **1989**, *56*, 237.
- (36) Cheng, H. N.; Ewen, J. A. *Makromol. Chem.* **1989**, *190*, 1931.
- (37) Collins, S.; Gauthier, W. J.; Holden, D. A.; Kuntz, B. A.; Taylor, N. J.; Wardt, D. G. *Organometallics* **1991**, *10*, 2061.
- (38) Mizuno, A.; Tsutsui, T.; Kashiwa, N. *Polymer* **1992**, *33*, 254.
- (39) Randall, J. C. In *Polymer Sequence Determination: Carbon 13 NMR Method*; Academic Press: New York, 1977.
- (40) Krigbaum, W. R.; Uematsu, I. *J. Polym. Sci., Polym. Chem. Ed., Part A* **1965**, *3*, 767.
- (41) Galante, M. J.; Mandelkern, L.; Alamo, R. G.; Lehtinen, A.; Paukeri, R. *J. Therm. Anal.* **1996**, *47*, 913.
- (42) In ref 28 only the fraction of stereo defects is explicitly given. However, it is stated that regio defects are also present. Hence, the 4.4 mol % defects serves as a lower limit to the total defect concentration.
- (43) We should note parenthetically that, after quenching thin films of all the poly(propylenes) from the melt to temperatures as high as about 60 °C, the so-called "smectic" form can develop.<sup>69</sup> However, we have also noted that the formation of this structure at the low crystallization temperatures depends on the film thickness. It can develop under rapid quenching conditions in films whose thicknesses are less than about 20  $\mu\text{m}$ . The thickness of the films used to obtain the X-ray diffractograms are about 0.5 mm, so that a slower heat transfer throughout the film allows the formation of well-defined  $\alpha$  type crystals.
- (44) Mezghani, K.; Phillips, P. J. *Polymer* **1998**, *39*, 3735.
- (45) Mezghani, K.; Campbell, R. A.; Phillips, P. J. *Macromolecules* **1994**, *27*, 997.
- (46) Fatou, J. G. *Eur. Polym. J.* **1971**, *7*, 1057.
- (47) Monasse, B.; Haudin, J. M. *Colloid Polym. Sci.* **1985**, *263*, 822.
- (48) Utilizing the equilibrium melting temperature that has been given for the  $\gamma$  form as a function of pressure,<sup>44</sup> the crystallizations at 125 MPa of the 1.26% polymer and the 1.7% polymer at atmospheric pressure are carried out at approximately the same undercooling.
- (49) Kalay, T.; Zhong, Z.; Allan, P.; Bevis, M. J. *Polymer* **1996**, *37*, 2077.
- (50) Randall, J. C. *Macromolecules* **1997**, *30*, 803.
- (51) Lotz, B.; Wittmann, J. C.; Lovinger, A. J. *Polymer* **1996**, *37*, 4979.
- (52) The degrees of crystallinity were calculated using the same heat of fusion for the  $\alpha$  and the  $\gamma$  forms. They have been reported to be similar.<sup>44</sup>
- (53) Mandelkern, L. *Crystallization of Polymers*; McGraw-Hill: New York, 1964.
- (54) Alamo, R. G.; Mandelkern, L. *Macromolecules* **1991**, *24*, 6480.
- (55) Flory, P. J. *Trans. Faraday Soc.* **1955**, *51*, 848.
- (56) Flory, P. J. *J. Am. Chem. Soc.* **1962**, *84*, 2857.
- (57) Voigt-Martin, I. G.; Mandelkern, L. *J. Polym. Sci., Polym. Phys. Ed.* **1981**, *19*, 1769.
- (58) Voigt-Martin, I. G.; Mandelkern, L. *J. Polym. Sci., Polym. Phys. Ed.* **1984**, *22*, 1901.
- (59) Meille, S. V.; Ferro, D. R.; Brückner, S. *Macromol. Symp.* **1995**, *89*, 499.
- (60) Voigt-Martin, I. G.; Alamo, R.; Mandelkern, L. *J. Polym. Sci., Polym. Phys. Ed.* **1986**, *24*, 1283.
- (61) Michler, G. H.; Brauer, E. *Acta Polym.* **1983**, *34*, 533.
- (62) Flory, P. J.; Yoon, D. Y.; Dill, K. A. *Macromolecules* **1984**, *17*, 862.
- (63) Yoon, D. Y.; Flory, P. J. *Macromolecules* **1984**, *17*, 868.
- (64) Flory, P. J. In *Principles of Polymer Chemistry*; Cornell University Press: Ithaca, NY, 1953.
- (65) Corradini, P.; Petraccone, V.; Pirozzi, B. *Eur. Polym. J.* **1983**, *19*, 299.
- (66) Mandelkern, L.; Fatou, J. G.; Howard, C. J. *Phys. Chem.* **1965**, *69*, 956.
- (67) The calculation can be carried out for other types of nucleation and different parameters. Although the values of  $\xi^*$  change, the trends with defect concentration and temperature remain essentially the same.
- (68) Brown, G. M.; Alamo, R. G.; Mandelkern, L., to be published.
- (69) McAllister, P. B.; Carter, T. J.; Hinde, R. M. *J. Polym. Sci., Polym. Phys. Ed.* **1978**, *16*, 49.

MA981849R